Dewetting of Star Nanogel/Homopolymer Blends from an Immiscible Homopolymer Substrate

Bin Wei,[†] Paul A. Gurr,[§] Jan Genzer,[†] Greg G. Qiao,*[,§] David H. Solomon,[§] and Richard J. Spontak*[,†,‡]

Departments of Chemical & Biomolecular Engineering and Materials Science & Engineering, North Carolina State University, Raleigh, North Carolina 27695, and Polymer Science Group, Department of Chemical & Biomolecular Engineering, University of Melbourne, Victoria 3010, Australia

Received July 6, 2004
Revised Manuscript Received August 26, 2004

The stability of polymer films is crucial to the success of numerous technologies, including adhesives, paints, and lithography. An imbalance between long-range van der Waals interactions acting across such films and short-range interactions restricted to the film/substrate and film/air interfaces is responsible for destabilizing the films, which is manifested by film dewetting from the substrate.[1−3] Most prior research endeavors have focused on elucidating the factors governing the dewetting mechanism and kinetics of a single hA homopolymer[4−8] or an AB diblock copolymer[9−13] on a solid or molten substrate. Several studies have likewise investigated the effects of nanoparticles,[14] dendrimers,[15] and nanostructured carbons[16] on thin film dewetting. Recently, we have examined the dewetting kinetics of AB/hA block copolymer/homopolymer blends on a molten hB substrate and have demonstrated[17] that the dewetting rate is sensitive to copolymer concentration and molecular weight disparity (M_A/M_{hA}). In this work, we report on the dewetting of an ultrathin polystyrene (PS) film containing nanogel (NG) particles, star-branched molecules[18,19] composed of a cross-linked divinylbenzene (DVB) core and poly(methyl methacrylate) (PMMA) arms, from the surface of a PMMA substrate. In this regard, the NG particles can be envisaged as permanent micelles and can be compared to dynamic block copolymer micelles capable of structural transformation in response to their environment.

The PS homopolymer (M_w = 50 kDa, M_w/M_n = 1.06) was provided by Pressure Chemical, Inc. (Pittsburgh, PA), whereas the PMMA homopolymer (M_w = 226 kDa, M_w/M_n = 1.04) and a poly(styrene-*b*-methyl methacrylate) (SM) diblock copolymer with 48 wt % S and M_w = 104 kDa (M_w/M_n = 1.04) was supplied by Polymer Source, Inc. (Dorval, Canada). All materials were used as-received. Solvent-grade toluene was supplied by Fisher Scientific (Fairlawn, NJ) and was used without further purification. The star NG was synthesized according to the "arms-first" procedure[18,19] wherein the PMMA arms were synthesized first by atom-transfer radical polymerization (ATRP) and then cross-linked with DVB to form discrete particles also under ATRP conditions. According to gel permeation chromatography (TriSEC) in THF, M_n and M_w of the NG were 335 and 370 kDa, respectively, and the gyration radius was about 13 nm. The number of PMMA arms, each with a molecular weight of about 11 kDa (M_w/M_n < 1.1), on a single NG particle was 28. A detailed description of the NG in the presence of PS and PMMA homopolymers, as well as the SM copolymer, is forthcoming.[20] Double-layer specimens for dewetting analysis were prepared by first spinning a 1.2 wt % solution of PMMA in toluene to a film thickness of ≈50 nm, as discerned from ellipsometry, on silicon wafers. Films of PS/NG or PS/SM blends varying in additive concentration were likewise spin-coated from toluene to a thickness of 66 nm on glass slides, scored with a razor blade and floated onto the surface of deionized water. Each film prepared in this fashion was subsequently picked up on the top of a PMMA-coated wafer, and the corresponding double-layer assembly was air-dried at ambient temperature for at least 24 h prior to annealing at 180 °C under nitrogen flow. The annealing temperature was chosen to be far above the glass transition temperatures (T_gs) of the PS (≈100 °C) and PMMA (≈120 °C at 79% syndiotacticity, as reported by the manufacturer).[21] Time-resolved optical microscopy images of the resultant films were acquired with an Olympus BX60 microscope equipped with a computer-interfaced CCD camera and operated in reflection mode. To discern the topography of the PS/PMMA interface, selected double-layer assemblies were promptly cooled from 180 °C to ambient temperature, far below the T_gs of both matrix homopolymers, so that the morphology of the assembly could be frozen-in. After the top PS layer was dissolved in cyclohexane (a selective solvent for PS), atomic force microscopy (AFM) images of the exposed PMMA substrate were collected with a Digital Instruments 3000 microscope operated in tapping mode with a Si_3N_4 tip.

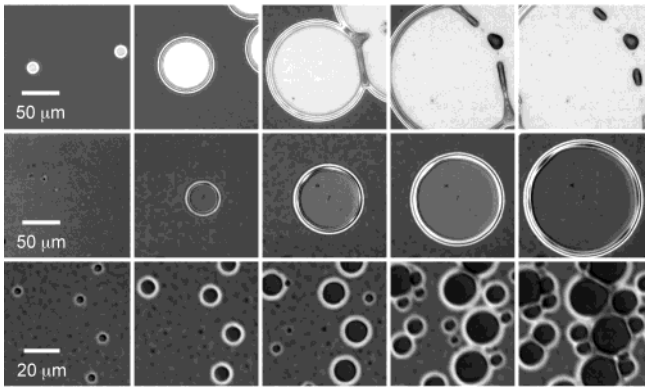

Figure 1. Time-resolved optical microscopy images (using phase-contrast and Nomarski optics) acquired from PS/PMMA double-layer assemblies possessing different concentrations of NG particles (in wt %) in the top PS layer: 0 (top row), 3 (middle row), and 20 (bottom row). The corresponding annealing times (in min) at 180 °C are 5, 30, 60, 90, and 120 in the top and middle rows but only 5, 10, 15, 20, and 25 in the bottom row.

Because of the intrinsic thermodynamic incompatibility between PS and PMMA at the annealing temperature (χN > 10)[22] and because the interfacial energy between PS and PMMA ($\gamma_{PS/PMMA}$ = 1.26 mJ/m^2 at 180 °C)[23] is larger than the difference in homopolymer surface tension ($\gamma_{PS} - \gamma_{PMMA}$, where γ_{PS} = 29.3 mJ/m^2 and γ_{PMMA} = 29.0 mJ/m^2),[24] the films spontaneously

[†] Department of Chemical & Biomolecular Engineering, North Carolina State University.
[‡] Department of Materials Science & Engineering, North Carolina State University.
[§] University of Melbourne.
* To whom correspondence should be addressed.

10.1021/ma048636o CCC: $27.50
Published on Web 10/12/2004

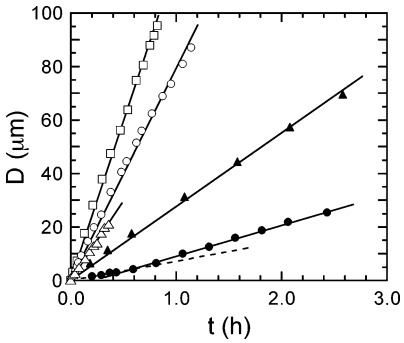

Figure 2. Dependence of hole diameter (D) on annealing time (t) at 180 °C for PS/PMMA double-layer assemblies containing different concentrations of NG particles (in wt %) in the top PS layer: 0 (□), 3 (○) and 20 (△). Included for comparison are data collected from assemblies with different concentrations of SM diblock copolymer (in wt %) in the top PS layer: 1 (▲) and 3 (●). The solid and dashed lines are linear regressions to the data, and the corresponding slopes yield the dewetting rate (dD/dt) discussed in the text.

dewet when annealed. The series of optical microscopy images shown in the top row of Figure 1 demonstrates the nucleation and growth of holes in the PS film with increasing annealing time. As the hole diameter increases, a rim that contains dewetted material begins to form around the hole. At long annealing times, neighboring holes may merge, which causes the rims to break into discontinuous islands due to Rayleigh instability.[25] Because the molecular weight of the PS is not very high and the thickness of the top PS layer is relatively thin (only about five molecular diameters thick, assuming Gaussian coils with a repeat unit length of 0.70 nm), the dewetting process is fast. When the NG is mixed into the top PS layer, the dewetting of the top layer slows considerably (cf. the images in the middle and bottom rows of Figure 1). The hole density (i.e., the number of holes per unit area) increases when the NG concentration in the PS matrix is increased from 3 (middle row of Figure 1) to 20 wt % (bottom row of Figure 1).

Quantitative analysis of the dewetting rate, expressed in terms of the time evolution of the hole diameter (dD/dt), has been performed by analyzing individual holes in images such as those displayed in Figure 1 with the Scion image analysis software package. The results, summarized in Figure 2, confirm that the neat PS dewets from the PMMA substrate at a relatively fast, constant rate ($dD/dt \approx 114$ μm/h). When 3 wt % NG is added to the top PS layer, dD/dt is reduced to 76 μm/h, assuming a linear $D(t)$ dependence (and no-slip conditions[26]) to permit quantitative comparison. The dewetting rate is further slowed to 59 μm/h when the NG concentration is increased to 20 wt %. The decrease in dD/dt due to the presence of NG in the top PS layer can be attributed to the migration of NG particles to the PS/PMMA interface, since the arms are chemically identical to the substrate but are immiscible in the PS matrix. Because the molecular weight of the NG arms (≈11 kDa) is more than an order of magnitude lower than that of the PMMA substrate (226 kDa), the thermodynamic incompatibility (χN) between the PS layer and the NG is substantially lower than that between the PS and the PMMA substrate. If the bilayered system nevertheless seeks to minimize its free energy by allowing the PMMA gels to migrate to the PMMA substrate, aggregation of NG particles at the PS/PMMA interface is expected to reduce the incompatibility between the two immiscible homopolymers. In other words, the NG particles effectively serve as surfactants, which promote a slower dewetting rate of the top PS/NG layer relative to that of the neat PS homopolymer. If this scenario accurately describes the system under investigation, then the presence of nanogel aggregates at the dewetted PS/PMMA interface should be amenable to experimental verification, as described in detail below.

While the dewetting rate is noticeably suppressed upon addition of NG particles to the top PS layer, the reduction in dewetting rate thus induced is not nearly as pronounced as that achieved via incorporation of the SM block copolymer.[17] Dewetting results measured for PS/SM films on the same PMMA substrate are included for comparison in Figure 2. Note that the dewetting rate of the PS/NG layer containing 20 wt % NG (59 μm/h) is more than twice that of a PS/SM blend with only 1 wt % of the copolymer (≈26 μm/h). This profound difference is understandable if one recalls that, unlike the SM micelles (which measure[17] about 40 nm in diameter in the present study), the NG particles are permanent in shape and never permit the PS matrix molecules to come into contact with the cross-linked DVB core. The micelles, on the other hand, can break and adsorb along the PS/PMMA interface, as discussed further below. Another observed difference between the dewetting of PS/NG and PS/SM blends on PMMA is that the dewetting rate of the PS/NG blend remains constant for NG concentrations as high as 20 wt %. In corresponding PS/SM layers, dewetting is found[17] to accelerate with increasing annealing time. This feature, while more distinct for PS/SM blends composed of high-molecular-weight PS, is evident, for instance, in the dewetting results obtained from the PS/SM blend with 3 wt % SM at $D \approx 6$ μm (see the intersection of the solid and dashed lines in Figure 2).

Figure 3a is an AFM image that verifies the PS/PMMA interface remains smooth (the rms roughness, R, is 0.36 nm) even after (i) addition of 3 wt % NG to the top PS layer and (ii) annealing for 2.5 h at 180 °C. Identical images are obtained from the PS/PMMA double-layer in the absence of NG.[17] In both cases, no difference is observed in the interfacial topography due to the occurrence of PS or PS/NG layer dewetting. That is, the interface remains equally smooth in specimen areas that dewetted (holes) and areas that remain intact (islands). In marked contrast, the interface between the layers becomes substantially roughened when 20 wt % NG is dispersed into the top PS layer. After only 30 min of annealing at 180 °C, large aggregates measuring on the order of 400−600 nm across become visible on the hole floor ($R = 2.62$ nm), signifying where the PS/NG layer dewetted from the PMMA substrate (cf. Figure 3b). The interfacial area remaining in contact with PS/NG islands, however, remains surprisingly smooth. After an additional 60 min of annealing, the PS/PMMA interface located under the islands also undergoes considerable roughening ($R = 3.97$ nm). At this annealing time and beyond, AFM images acquired from the hole floor and under the PS/NG islands are not distinguishable, as indicated by Figure 3, parts c and d. Such roughening, as well as the measured reduction in dewetting rate, can be explained in terms of the spatial position of the NG particles within the double-layer assembly.

As mentioned earlier and illustrated in Figure 4a, the chemical incompatibility between PMMA and PS triggers the migration of NG particles toward the PMMA substrate. Because of its relatively short arms, the NG

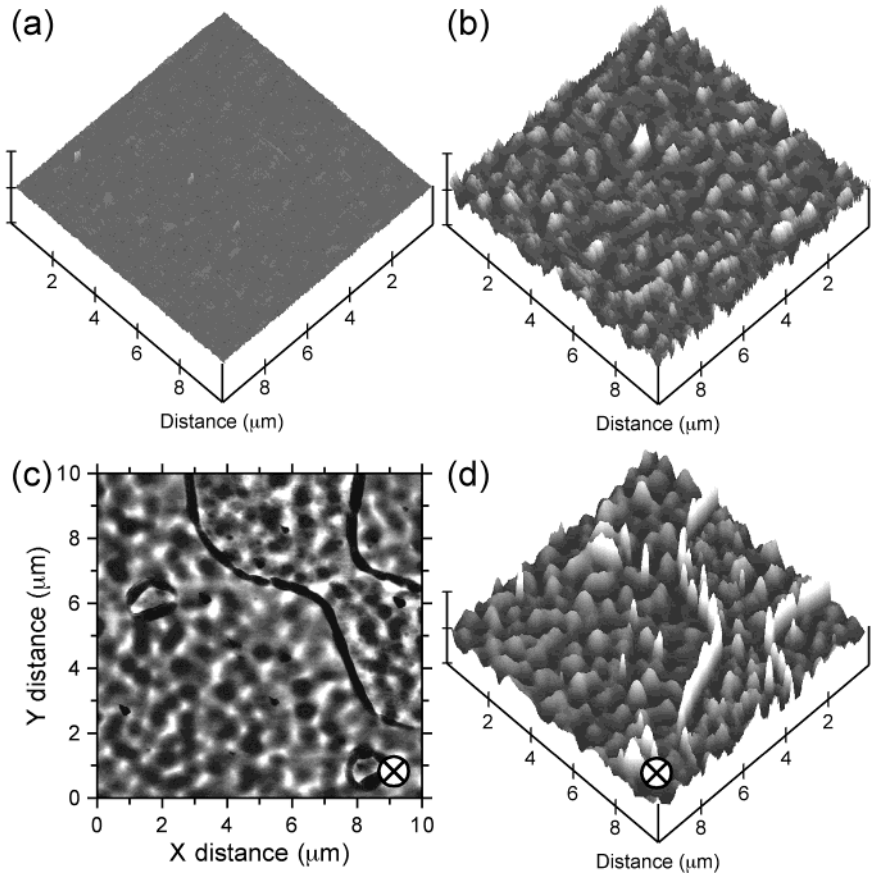

Figure 3. Representative height (a, b, d) and phase (c) AFM images of the PS/PMMA interface in double-layer assemblies upon annealing for a time (t) at 180 °C, followed by selective solvent removal of the top PS layer. In part a, the interface at a dewetted hole (t = 2.5 h) appears smooth even though the top PS layer contains 3 wt % NG. In parts b−d, specimens incorporating 20 wt % NG are displayed. The image in part b is collected from a hole (t = 30 min) and appears rough, whereas those displayed in parts c and d are obtained from a PS island, located between the dark lines evident in part c, and an adjacent hole (t = 90 min). Each image measures 10 μm across, and the scan height is 20 nm/division.

acts as a surfactant at the interface between the two immiscible polymer layers, which leads to improved film stability and decreased dewetting rate. Since the NG core is cross-linked and the arms are permitted to dangle, it is reasonable to visualize the NG particles as permanent micelles with a dense coronal brush composed of PMMA arms. The relatively high molecular weight of the PMMA molecules comprising the substrate entropically prohibits their penetration into, and wetting of, the NG coronal brush due to the high grafting density of arms. This so-called autophobic effect[27] does not allow the NG particles to sink into the PMMA substrate once they reach the PS/PMMA interface. Depending on the NG concentration in the PS matrix, two possible arrangements of NG particles at the PS/PMMA interface are depicted in Figure 4a. At low NG concentrations (e.g., 3 wt % NG), the interface remains smooth, confirming that no significant NG aggregation occurs. This NG concentration is presumably too low for individual NG particles to interact to a significant extent with each other.

Increasing the NG concentration of the nanogel in the top PS layer, however, leads to a markedly different scenario. After annealing the specimen with 20 wt % NG for 30 min, aggregates are observed on the hole floor, but are absent from the interfacial area covered by PS islands. At longer annealing times, NG aggregates are evident in both areas (cf. Figure 3, parts c and d). Segregated from the PS matrix and relocated in the limited space across the PS/PMMA interface, the NG particles at this concentration are in sufficiently close contact with one another to permit extensive penetration of the arms (comprising the coronal brush) on neighboring NG particles, which would promote considerable aggregation at the PS/PMMA interface, as well as in the top PS layer.[19] Dynamic SM copolymer micelles likewise migrate to the PS/PMMA interface (cf. Figure 4b). Because of their innate ability to structurally transform in response to their surrounding environment, however, they can break and spread out upon reaching the PS/PMMA interface to form isolated copolymer mushrooms or, at high copolymer concentrations, a planar brush along the interface with no discernible change in surface roughness (data not shown). Moreover, as the top PS-rich layer dewets from the PMMA substrate, block copolymer molecules located near the PS/PMMA interface can likewise form low-density brushes capable of interpenetrating with and entangling the PS chains.[28] In both instances, enthalpic considerations arising from the immiscibility of the S block of the copolymer and the PMMA substrate are principally responsible for locating the copolymer molecules along the interface, which explains why the addition of copolymer is so much more effective at inhibiting polymer−polymer dewetting.

In summary, incorporation of NG particles, star-branched molecules envisaged as permanent micelles, into the top PS layer serves to decrease the growth rate of holes as the PS layer dewets from the PMMA substrate. The dewetting rate is systematically reduced

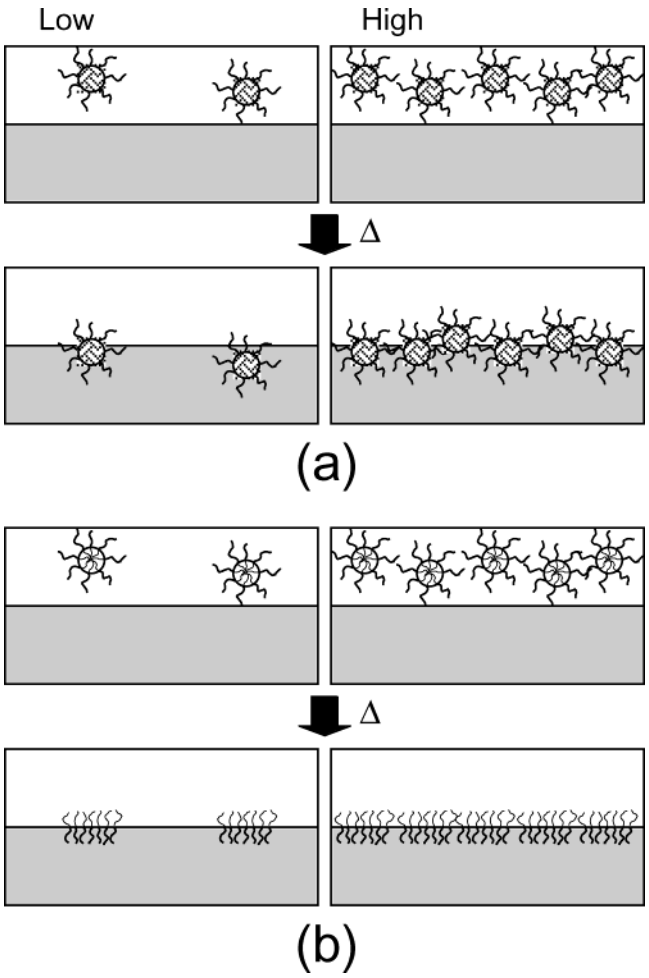

Figure 4. Schematic illustration of the mechanisms by which (a) NG particles and (b) block copolymer micelles residing in the top polymer layer reduce the rate at which the top layer dewets from the bottom polymer layer. In part a, we assume that the dangling arms comprising the coronal brush are much lower in molecular weight than the substrate polymer to ensure autophobicity so that the NG particles locate at the polymer−polymer interface.

by increasing the NG concentration over the concentration range examined and is attributed to thermodynamically driven migration of NG particles to the PS/PMMA interface. At sufficiently high NG concentrations, the NG particles aggregate in the top PS layer, as well as at the PS/PMMA interface. Due to the molecular weight disparity between the PMMA arms comprising the NG particles and the PMMA molecules in the substrate, autophobicity restricts the NG particles to remain at the interface and serve as compatibilizing agents. This mechanism of interfacial compatibilization differs markedly from that of dynamic block copolymer micelles, which are capable of breaking and spreading out into copolymer mushrooms or, at sufficiently high copolymer concentrations, a monolayer (brush) along the PS/PMMA interface.

Acknowledgment. This work was supported by the Kenan Institute for Engineering, Technology and Science at North Carolina State University, and a Linkage-International project sponsored by the Australian Research Council (G.G.Q. and R.J.S.).

References and Notes

(1) Brochard-Wyart, F.; Debregeas, G.; Fondecave, R.; Martin, P. *Macromolecules* **1997**, *30*, 1211 and references cited therein.
(2) Geoghegan, M.; Krausch, G. *Prog. Polym. Sci.* **2003**, *28*, 261.
(3) Kaya, H.; Jérôme, B. *Eur. Phys. J. E* **2003**, *12*, 383.
(4) Faldi, A.; Composto, R. J.; Winey, K. I. *Langmuir* **1995**, *11*, 4855.
(5) Krausch, G. *J. Phys.—Condens. Matt.* **1997**, *9*, 7741.
(6) Wang, C.; Krausch, G.; Geoghegan, M. *Langmuir* **2001**, *17*, 6269.
(7) Lambooy, P.; Phelan, K. C.; Haugg, O.; Krausch, G. *Phys. Rev. Lett.* **1996**, *76*, 1110.
(8) Masson, J. L.; Green, P. F. *Phys. Rev. Lett.* **2002**, *88*, 205504.
(9) Segalman, R. A.; Green, P. F. *Macromolecules* **1999**, *32*, 801. Masson, J. L.; Green, P. F. *J. Chem. Phys.* **2000**, *112*, 349.
(10) Costa, A. C.; Composto, R. J.; Vlcek, P. *Macromolecules* **2003**, *36*, 3254.
(11) Muller-Buschbaum, P.; Gutmann, J. S.; Lorenz-Haas, C.; Wunnicke, O.; Stamm, M.; Petry, W. *Macromolecules* **2002**, *35*, 2017.
(12) Hamley, I. W.; Hiscutt, E. L.; Yang, Y. W.; Booth, C. *J. Colloid Interface Sci.* **1999**, *209*, 255.
(13) Leonard, D. N.; Smith, S. D.; Russell, P. E.; Spontak, R. J. *Macromol. Rapid Commun.* **2002**, *23*, 205. Leonard, D. N.; Spontak, R. J.; Smith, S. D.; Russell, P. E. *Polymer* **2002**, *43*, 6719.
(14) Sharma, S.; Rafailovich, M. H.; Peiffer, D.; Sokolov, J. *Nano Lett.* **2001**, *1*, 511.
(15) Mackay, M. E.; Hong, Y.; Jeong, M.; Hong, S.; Russell, T. P.;, Hawker, C. J.; Vestberg, R.; Douglas, J. F. *Langmuir* **2002**, *18*, 1877.
(16) Barnes, K. A.; Karim, A.; Douglas, J. F.; Nakatani, A. I.; Gruell, H.; Amis, E. J. *Macromolecules* **2000**, *33*, 4177.
(17) Wei, B.; Genzer, J.; Spontak, R. J. *Langmuir*, in press.
(18) (a) Solomon, D. H.; Qiao, G. G.; Abrol, S. Process for Microgel Preparation. WO 99/58588, 1999 (The University of Melbourne). (b) Gurr, P. A.; Mills, M. F.; Qiao, G. G.; Solomon, D. H. *Macromolecules*, Submitted for publication.
(19) Gurr, P. A.; Qiao, G. G.; Solomon, D. H.; Harton, S. E.; Spontak, R. J. *Macromolecules* **2003**, *36*, 5650.
(20) Gurr, P. A.; Wei, B.; Genzer, J.; Solomon, D. H.; Spontak, R. J.; Qiao, G. G. Manuscript in preparation.
(21) Brandrup, J., Immergut, E. H., Grucke, E. A., Eds. *Polymer Handbook*, 4 ed.; Wiley & Sons: New York, 1999.
(22) Balsara, N. P. In *Physical Properties of Polymers Handbook*; Mark, J. E., Ed.; AIP Press: New York, 1996; Chapter 19.
(23) Harris, M.; Appel, G.; Ade, H. *Macromolecules* **2003**, *36*, 3307.
(24) Wu, S. *Polymer Interface and Adhesion*; Marcel Dekker: New York, 1982.
(25) Sharma, A.; Reiter, G. *J. Colloid Interface Sci.* **1996**, *178*, 383.
(26) Insufficient early-time data are available to distinguish between slip ($D \sim t^{2/3}$) and no-slip ($D \sim t$) conditions. For a detailed discussion of this topic, the interested reader is referred to: Jacobs, K.; Seemann, R.; Schatz, G.; Herminghaus, S. *Langmuir* **1998**, *14*, 4961.
(27) Borukhov, I.; Leibler, L. *Phys. Rev. E* **2000**, *62*, R41.
(28) Oslanec, R.; Costa, A. C.; Composto, R. J.; Vlcek, P. *Macromolecules* **2000**, *33*, 5505.

MA048636O